CHAPTER I

INTRODUCTION

Gene discovery

To test a hypothesis, the idea may be approached from various angles. Multiple, independently designed experiments are performed and a conclusion is drawn based on all results. Therefore, when we ask a general question such as, "what causes heart disease?" we are obligated to approach the issue from multiple perspectives, such as environment vs. genetics. If we choose to investigate the genetic standpoint, then there are a variety of genetic approaches we can select. For example, we can start with the diseased individuals and chisel our way down to the gene function. Or we can start from the bottom, pinpointing a gene and work up to the function on the organismic level. When our laboratory made an attempt to examine a cause of developmental heart malformations, we chose the latter approach.

Gene discovery is both exciting and frustrating because although all discoveries are novel, the sheer uncertainness and lack of supporting evidence requires perseverance. An initial step in determining the function of a novel gene is to analyze the cDNA sequence to identify any known domains or sequence homology. Next, it is imperative to examine the RNA or protein expression pattern. A hypothesis can be formulated based on known features that all gene expressing tissues or cell populations share. Experiments can then be designed to examine specific processes involved in the predicted function. In an attempt to examine genes that are involved in heart formation, we designed a subtractive hybridization that would isolate genes that are specifically expressed in the heart. The PCR-based screen was performed on HH stage 18

chick, which is a critical time during heart development, and produced 12 novel gene fragments. For my thesis project, I have worked on determining the function of two of these genes - *hole* and *bves*.

Cell adhesion in development

Unpredictability prevailed, and both *bves* and *hole* expression were not restricted to the heart throughout embryogenesis. Instead, *hole* was additionally expressed in the chick brain and neural tube, and expression in the mouse completely excluded the heart but included brain and limb tissue. The lack of consistent pattern across species and the inability to develop immuno-specific antibodies against Hole protein resulted in discontinuation of the *hole* study. The second gene of interest, *bves* also is additionally expressed in a number of non-cardiac epithelial derived tissues. Expression patterns in the frog, chick, and mouse are consistent, and we have developed many tools that have facilitated us in investigating *bves* function. Fortunately, in the case of *bves* isolation, the risk of gene discovery was beneficial and the *bves* studies not only furthered the understanding of epicardium and coronary artery development, but a new class of cell adhesion molecules was defined and several developmental processes that require *bves* were identified.

What impact does cell-cell adhesion have on development? Cell-cell junctions are specialized structures that are essential for both intercellular adhesion and communication. During development, adhesion molecules play important roles in overall tissue organization and morphogenesis. The most basic element of cell-cell adhesion is the physical bond between two or more cells, maintaining the structural integrity of an embryo. A classic example of the importance of cell adhesion sustaining structural integrity is during *X. laevis* embryo cleavage. Two cell adhesion molecules, XB/U- and EP/C-cadherin are expressed on all newly formed cell

membranes and are responsible for keeping the blastomeres together until gastrulation (Angres et al., 1991; Heasman et al., 1994b). If antisense primers against EP/C-cadherin are introduced into the oocyte, the resulting blastomeres display loss of cell-cell adhesion and the blastocoel is obliterated (Heasman et al., 1994b).

As cells proliferate and differentiate, cell recognition and cell sorting are vital to segregate cells into distinct tissue layers or compartments. Dynamic expression of the various cadherins is primarily responsible for cell condensation and sorting of various tissues, such as neural (N-cadherin) and epithelial (E-cadherin) tissues. Proper cell morphogenesis often requires extensive cell rearrangement and migration. Cells migrating as an adherent group require a delicate balance of cell-cell adhesion for cells to move past surrounding cells and cell adherence with the migrating group. During *X. laevis* gastrulation ectodermal cells undergo a cell rearrangement called convergent extension and migrate together as an epithelial sheet as they cover the vegetal yolk cells in a process called epiboly. These cells remain an adherent epithelium as they involute into the blastopore lip and travel along the archenteron roof. EP/C- and E-cadherin maintain proper adhesion between gastrulating *X. laevis* cells involved in tissue elongation and convergence extension movements associated with involution (Lee and Gumbiner, 1995; Levine et al., 1994). EP/C-, XB/U-, E-, and N-cadherin are expressed at different times and amongst different cell populations during cleavage, gastrulation, and neurulation for the purpose of cellular adhesion and cell sorting that allows for proper cell arrangement and migration.

Gastrulation involves the coordination of several distinct events driven by region-specific movements that are associated with a complex balance of spatially and temporally regulated adhesion. The beginning of gastrulation is marked by changes in shape of bottle cells at the site

of the blastopore (Diagram 1A). These endodermal bottle cells invaginate in the marginal zone, permitting the marginal cells to involute through the blastopore lip and continue to pass into the interior as a sheet. The involuting cells at the leading edge of the mesodermal mantle migrate along the inner surface of the blastopore roof towards the animal pole, forming the archenteron or primitive gut (Diagram 1B-C). These sets of movement are driven by active repacking of the cells, where cells cooperatively form and align lamellipodia creating interdigitation of cells, and resulting in narrowing and elongation of tissue (Keller et al., 1992; Wilson et al., 1989). This forms the force necessary for the cells to converge

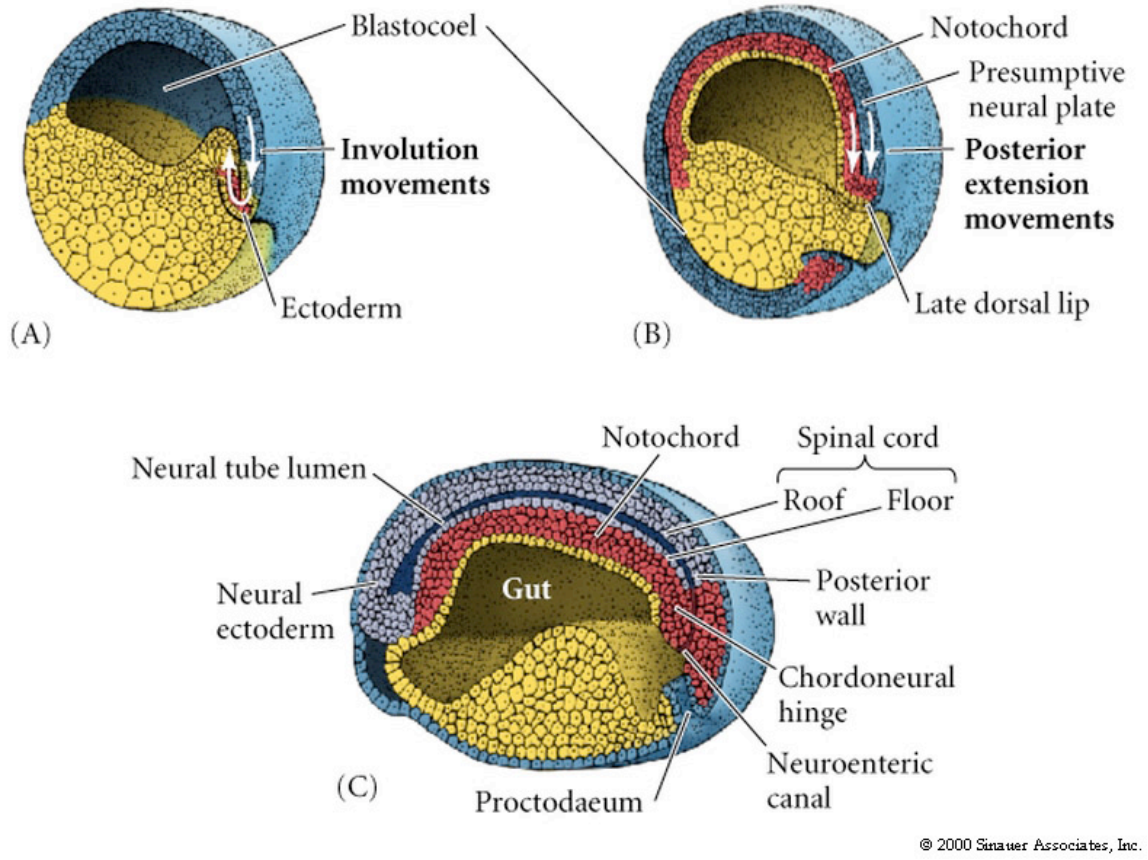

Diagram 1. Gastrulation movements during *X. laevis* embryogenesis. Cross section of an *X. laevis* embryo during early (A), mid (B), and late (C) gastrulation. The direction of cell movements are indicated by the white arrows.

toward the dorsal midline and extend along the antero-posterior axis, also known as convergent extension. During this time, the external epithelium in the region of the animal pole spreads to take the place of the cell sheets that have turned inward (Keller et al., 1992; Keller and Tibbetts, 1989; Wilson et al., 1989). The epithelium of the animal hemisphere extends to cover the entire external surface of the embryo. This mechanism of epiboly is driven by an increase in cell number coupled with change of cell shape and integration of several deep layers into one (Keller and Tibbetts, 1989; Keller, 1980). Dynamic expression of many types of adhesion molecules is associated with these three sets of movement during gastrulation. Migrating mesodermal cells on the blastocoel roof express integrins that bind to the extracellular matrix protein, fibronectin, covered along the roof (Beddington and Smith, 1993; Winklbauer, 1990). Cells undergoing convergent extension in the marginal zone express EP/C-cadherin and XB/U-cadherin (Levine *et al*. 1994; (Lee and Gumbiner, 1995), while the epiboly of the ectoderm depends upon E-cadherin (Levine et al., 1994). Therefore, we can conclude that cell adhesion molecules play a role in cell movements, both in cell adhesion and cell detachment, during early *X. laevis* embryogenesis that are vital for the proper formation of the three germ layers and continued normal development.

Gastrulation is just one of many developmental events in which cell adhesion plays an essential role. Neurulation and organogenesis are also processes that are vital to the development of an organism and proper cell-cell adhesion allows for these events to be carried out correctly. The example that I have used to illustrate the adhesive role of *bves* plays in organogenesis is eye development. Retina, lens, and cornea formation all require movement and reshaping of epithelia, as does corneal regeneration. Specifically, the optic vesicle is formed from a lateral outpocketing of the diencephalon. The retina is developed from the invagination of the optic vesicle resulting in the two epithelial layers facing each other, and ultimately fusing

together to form the multi-layered retina. The lens and cornea are formed from a thickening of surface epithelia into a multi-layered placode. In the case of the lens, the thick placode detaches from the surface and drops down into the optic cup space. The anterior epithelium remains proliferative, as the posterior epithelium differentiates into lens fiber cells. The corneal epithelium is derived from a single cell layer and stratifies into a five-cell layer thick structure, while neural crest cells migrate under the corneal epithelium and produce the corneal stroma. There are a limited number of studies documenting which adhesion molecules participate in the formation of these three critical eye structures, however, a mechanistic understanding of how cell adhesion regulates this complex series of morphogenetic movements is lacking.

A second function of cell adhesion molecules is signal transduction in pathways that regulate a variety of cell process, including cell association, motility, cell growth, apoptosis and gene regulation. The Wnt pathway is a well-studied signaling cascade that is implicated in developmental patterning processes (Huelsken et al., 2000; Klingensmith and Nusse, 1994; Larabell et al., 1997; Maloof et al., 1999; Schneider et al., 1996). The cadherin-associated cytoplasmic protein armadillo/ß-catenin controls Drosophila segment polarity (McCrea et al., 1991; Peifer and Wieschaus, 1990; Wieschaus et al., 1984) and induces the dorsal-ventral and anterior-posterior body axes in *X. laevis* (Funayama et al., 1995; Guger and Gumbiner, 1995; Heasman et al., 2000; Montross et al., 2000). The association of ß-catenin with the C-terminal tail of cadherin family members is crucial for cell-cell adhesion regulated by homotypic binding of cadherins (Aberle et al., 1994; Nagafuchi and Takeichi, 1989; Ozawa and Kemler, 1992). Therefore, there are two events, cadherin-mediated cell adhesion and the Wnt signaling pathway, that are competing for the same pool of armadillo/ß-catenin. This provides evidence that

suggests that cadherin-mediated cell adhesion is linked to these signaling and developmental patterning events (Heasman et al., 1994a).

Bves family

There have been a handful of documented studies on *bves* expression patterns and possible *in vitro* function published by past and present members in our laboratory and from other groups (Andree et al., 2002; Andree et al., 2000; Reese and Bader, 1999; Reese et al., 1999; Wada et al., 2001). Although there has been no link of *bves* to any known signaling pathways, investigation of *bves* function is in its initial stages and we cannot rule out any possibilities. The number of unanswered questions is often a caveat of gene discovery, but it is important to consider all possible scenarios. Collectively, studies have determined that *bves* (also called *pop1* by Andree et al., 2000) is a novel family that shares no protein homology to any other gene product and has no known functional domains. To date, there are three family members in chick, two in human and mouse, and one each in *X. laevis* and *Drosophila* (Andree et al., 2000; Hitz et al., 2002; Reese and Bader, 1999; Reese et al., 1999). Bves1 (referred to as Bves for the remainder of this document) has three transmembrane domains with a long C-terminal tail and short N-terminus. Two highly conserved asparagine-linked glycosylation sites have been identified in the N-terminus and shown to be glycosylated *in vitro* and *in vivo* (Knight et al., 2003). Additionally, oligmerization of Bves molecules in COS cells and in chick heart explants are detected by Western blot analysis under nonreduced conditions (Knight et al., 2003; Vasavada et al., 2004). Antisera developed against Bves in chick show a dynamic cellular distribution of the protein in cells that migrate from the proepicardial organ to form the epithelial epicardium and further to form the smooth muscle of the coronary arteries. In the freely

migrating mesenchyme, localization of Bves protein is cytoplasmic. Upon epithelial assembly, Bves translocates to the cell surface where it maintains a strong expression pattern (Reese et al., 1999; Wada et al., 2001). Immunocytochemical studies in epithelial cell cultures of MDCK, rat epicardial cells, and A6 *X. laevis* kidney epithelial cells have supported this same dynamic Bves expression pattern (Osler and Bader, 2004; Ripley and Bader, unpublished data).

RT-PCR, Northern blot analysis, and whole mount *in situ* hybridization data have indicated that *bves* is expressed in a variety of embryonic tissues including heart, skeletal muscle, gut, brain, spleen, and kidney (Andree et al., 2000; Hitz et al., 2002), suggesting a general function amongst the development of these various organs. *In vitro* studies have isolated a homophilic binding domain (BD) in the C-terminal tail of Bves (Kawaguchi, unpublished data) and biochemical analysis has suggested that Bves-Bves interactions occur in the cytoplasm (Knight et al., 2003). Additionally, L-cells transfected with *bves* display calcium independent adhesiveness in the hanging drop assay (Wada et al., 2001). The current model of Bves structure includes three transmembrane regions, an extracellular glycosylated N-terminus, and an intracellular C-terminus (Figure 1). Bves molecules interact homophilically through the binding domain located in the cytoplasmic tail. Studies are underway to determine whether there are any extracellular N-terminus interactions and whether there are other C-terminus binding partners that facilitate Bves function. To date, however, there has been no *in vivo* data that designates the function of Bves.

Dissertation outline

The purpose of this dissertation is to describe the studies performed in an attempt to determine the function of two gene products, *hole* and *bves,* isolated from the subtractive

hybridization described earlier. The first chapter in this document outlines the cloning and expression pattern of *hole* in chick and mouse. I first cloned the chick sequence since the subtractive hybridization was performed in that species. I next chose to clone the mouse sequence for the future generation of *hole* null mice and related experiments. Structural analysis determined that the Hole protein was a six-transmembrane spanning protein that shared no known homology with any other gene family. Spatio-temporal expression pattern of *hole* mRNA was determined by whole mount *in situ* hybridization in both species. As mentioned above, the expression pattern differed extensively including strong expression in the chick heart throughout development versus no heart expression in the mouse. I was unable to develop Hole specific antiserum to determine the protein expression pattern or protein interactions by Western analysis. Lack of homology with other protein or functional domains proved difficult to elucidate function or design exploratory experiments and therefore, I decided to terminate this project. I should note that others have requested to continue this line of investigation and are determining the genetic locus of this gene.

The second chapter describes the cloning, expression, and morpholino knock-down experiments performed on the only *bves* family member known in the *X. laevis*. The purpose of cloning and examining *Xbves* in this model to determine function is detailed in chapter 3. Briefly, examination of the EST database revealed expression of a *bves* family member in the *X. laevis* at various developmental stages, including cleavage and gastrulation. Gastrulation represents a stage where various cell sorting and morphogenetic events are occurring, and unlike chick gastrulation, cells migrate together as an epithelial sheet in this process. Additionally, cell movements, cell fates, and signaling transduction cascades have been well documented during *X. laevis* gastrulation. With this established foundation, experimental design proved to be

straightforward and experiments to test protein function were more easily elaborated. The *X. laevis* and morpholino technology provided a quick and effective way to decrease amounts of Bves protein and examine resulting embryonic phenotypes. By utilizing *X. laevis* morpholino injection, I am able to acquire a *X. laevis* embryo lacking Xbves protein in one day compared to the many months required to develop a null mouse model. Using this system and information, I showed that *Xbves* was expressed at the cell surface of migrating epithelial cells during gastrulation. In embryos depleted of Xbves protein, epiboly movement was inhibited and gastrulation was unable to proceed. I next examined the expression of two well-studied genes, *goosecoid* and *Xbra*, involved in tissue organization and differentiation. The expression of these genes was not affected in embryos lacking Xbves protein, however the proper migration of these gene-expressing cells was inhibited. While future studies may place *Xbves* in a signal pathway, these studies did not show an *Xbves* exhibiting an affect on expression of these markers.

The third chapter of this dissertation reports the spatio-temporal expression pattern of *bves* during eye morphogenesis and describes a potential function of *bves* during corneal repair. The purpose of this study was to demonstrate how vast and vital *bves* function is throughout embryogenesis. The eye serves as an excellent model of organogenesis, whose differentiation has proven to be dependent on proper expression and function of cell adhesion molecules, as well as representing a system with a dynamic series of morphogenetic movements. In an attempt to illustrate *bves* function in the eye system, growth and repair of an immortal human corneal epithelial cell line was analyzed with and without morpholino treatment. While future functional studies need to be done in the embryo, this chapter is the first demonstration of *bves* expression in the eye, and morpholino treatment of corneal cells support our *X. laevis* findings that Bves is

essential in maintaining a critical balance of adhesion required in migrating and morphogenetic cell processes.

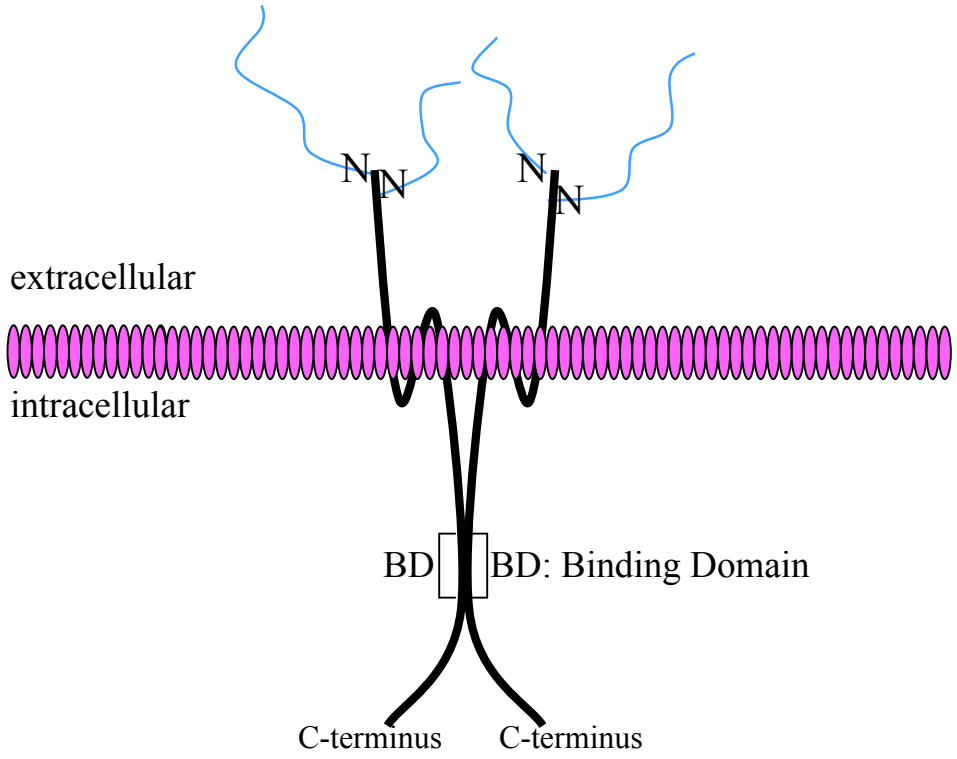

Figure 1. Schematic illustration of the predicted structure and topology of Bves. Bves is a three transmembrane protein with an intracellular C-terminus and two N-glycosylation sites N-terminus. This diagram depicts a Bves dimer interacting at the intracellular binding domain (BD).

In summary, I will introduce two novel genes isolated by my laboratory. I will show that though sometimes frustrating, the benefits of gene discovery are invaluable. Bves, a novel family of cell adhesion molecules have been identified and my dissertation will be the first illustration of a function of this molecule *in vivo*. Furthermore, in designing my experiments, I used model systems that were most advantageous to applying technologies either *in vivo or in vitro* in order to address my hypothesis. I used *X. laevis* embryos to examine epithelial movement during gastrulation, the chick embryo to determine Bves expression during ocular

formation, and a human corneal epithelial cell line to investigate the role of Bves in corneal regeneration. Collectively, I have shown that Bves plays a role in epithelial migration and morphogenetic cell processes.

CHAPTER II

ISOLATION AND EXPRESSION OF *HOLE*

Introduction

Gene discovery has proven to be very beneficial in both advancing our understanding of normal biological processes and in treatment of diseases caused by genetic mutations (Curran, 1998; Freeman, 2000; Ruccione, 1999; Wang and Feuerstein, 1997). Our goal in performing a heart specific subtractive hybridization was to isolate novel genes and study their function in heart formation (Reese et al., 1999). While this study on one of the novel genes isolated from the screen, called *hole,* did not yield exceptionally informative or mechanistic data, it is the first report of the isolation of this gene and illustration of a unique expression pattern. Still, others have already used these data to advance their own work on this topic.

This report will show an exceptionally high degree of homology of Hole amino acid sequence amongst chick, mouse, and human. Sequence analyses predict that Hole is a six-transmembrane protein with a long C-terminal tail. This membrane spanning structure of Hole resembles the configuration of cardiac ion channels. Strong expression of *hole* mRNA is detected in the chick heart and specific neural tissues. Analysis of *hole* in mouse detects no expression in heart, but a robust signal is found in the neural tube and brain. While this discrepancy may be due to detection of different family members or isoforms, I was only able to isolate one single cDNA from both chick and mouse libraries. However, I only performed these experiments with the selected resources and libraries reported here. Although the expression pattern of *hole* between chick and mouse is quite diverse, a similar feature between myocytes

and neurons is that both are electrically coupled cell types and can undergo spontaneous depolarization.

Analysis of *hole* demonstrates the difficulties of gene discovery and how it can lead to any number of new directions. The dynamic expression pattern and conserved sequence suggest a distinctive function in these organisms and others. Collectively, we can formulate a hypothesis based on the high homology of Hole across species, the similarity to ion channel structure, and the *hole* mRNA expression pattern in chick and mouse. From these date we can predict that *hole* may define a novel family of ion channels important in electrically coupled tissues. However, I have not tested this hypothesis and further studies are needed to determine the significance of *hole* in these processes.

Materials and Methods

cDNA library construction and screening

A chick stage 18 heart-subtracted library was constructed using PCR Select (Clontech) according to the manufacturer's instructions. cDNA from heart and heartless embryos was synthesized from poly-A RNA. The cDNA was *RsaI* digested and different adapters were ligated to two pools of the heart cDNA. The two adapter-ligated pools of heart cDNA and non-adapter heartless embryonic cDNA were hybridized separately, resulting in enrichment of differentially expressed sequences. A second round of hybridization between the two hybridized pools was performed in order to provide a template for PCR amplification using adapter-specific primers. After amplification, the differentially expressed cDNAs were cloned into the T-easy vector (Promega) and sequenced.

Cloning of chick and mouse *hole*

A stage 11 chick embryonic heart library was screened using 200 bp probe amplified from the original clone produced by the screen. Two separate clones were isolated and sequenced. The clone sizes were 1.48 kb and 3.12 kb sharing 1.01 kb overlapping sequence.

Mouse ESTs were identified by searching the NCBI EST databases. These sequences were then used to produce a 200 bp probe, which was in turn used to screen an embryonic day 14 mouse heart library (Stratagene). The screen yielded two separate clones of 1.6 kb and 2.8 kb. The larger clone had a poly A site 1.6 kb and 2.8 kb downstream and was determined to be a chimeric clone based on genomic sequence.

A chick genomic cosmid library was screened using a chick cDNA probe and yielded a >10,000 kb insert. The clone was sequenced and shown to contain the entire cDNA sequence in an intronless genomic structure.

A mouse lambda genomic library was also screened using a mouse cDNA probe yielding a >10,000 kb clone. The clone was sequenced and shown to contain all but 27 bp 5' of the cDNA sequence in a single exon. Additional mouse genomic sequence was accessed from NCBI BLAST database, which revealed a 27 bp exon 2 kb upstream of the 1.57 exon.

Sequence analysis

Protein translation and sequence analysis were performed using MacVector 6.5 (Oxford Molecular Group). Transmembrane prediction was based on a Markov model for predicting transmembrane helices executed by the TMHMM server provided by the Center for Biological Sequence Analysis.

Northern blot analysis

Total mRNA was isolation from various chick tissues using Trizol reagent (Life Technologies). Equal amounts (10 µg) were loaded onto a 6% formaldehyde denaturing gel for electrophoresis. RNA was transferred onto a positively charged nylon-based membrane (Genescreen Plus, DuPont) overnight and UV crosslinked. The membrane was prehybridized in Rapid Hyb-buffer (Amersham) at 65°C for 4 hours and then hybridized with a random-primed (redi-prime II, Amersham) 200 bp cDNA probe labeled with ^{32}P, overnight at 65°C. The blot was washed in a 2X SSC, 0.1% SDS buffer at 65°C and exposed to autoradiography overnight.

Whole mount *in situs*

RNA probes were transcribed and digoxygenin-UTP labeled from the open reading frame (orf) and 3'UTR of both chick and mouse cDNAs using T7 polymerase for the antisense probe and SP6 or T3 polymerase, for the sense probe. Embryos were fixed overnight in 4% paraformaldehyde and dehydrated in a methanol series for storage. For hybridization, embryos were rehydrated in a methanol/PBT series and treated with 10 µg/ml proteinase K for variable times (0-20 minutes). The embryos were post-fixed in 4% paraformaldehyde/0.2% gluteraldehyde for 20 minutes and then pre-hybridized in 50% formamide, 5X SSC, 1% SDS, heparin and tRNA for 2 hours at 70°C. Embryos were hybridized with sense and antisense probes in the prehybridization buffer at 70°C overnight. After a series of 50% formamide, 2-5X SSC, 0.5-1% SDS washes, embryos were pre-blocked in 10% heat inactivated-sheep serum in TBST/levamisole and incubated with a pre-absorbed anti-digoxygenin antibody (Roche) at a dilution of 1:2000 overnight at 4°C. Embryos were washed in TBST/levamisole for 5 hours and then treated with BM Purple Substrate (Roche) to produce color from the hybridized probe.

Radioactive *in situs*

RNA probes were transcribed and ^{35}S-methionine labeled from the same cDNAs described above. Embryos were paraffin embedded and sectioned at 7 microns. Sections were affixed onto slides and rehydrated in a PBS/ethanol series. Slides were fixed in 4% paraformaldehyde and proteinase K (20 µg/ml) treated for 7.5 minutes. After a 4% paraformaldehyde fix, slides were treated with 1-2 ml acetic anhydride in 0.1M triethanolamine for 20 minutes and dehydrated in an ethanol series. The probe was diluted in a 50% formamide, 10% dextran sulfate hybridization mixture to a final concentration of $2x10^4$cpm, applied dropwise onto the sections, and coversliped overnight. Slides were washed in 50% formamide, 2X SSC, 20mM 2-mercaptoethanol and RNase treated. Slides were dipped in emulsion (Kodak) and developed 5 days later using standard methods. Tissues were eosin-stained for visualization.

Results

Cloning of chick and mouse *hole*

A PCR-based subtractive hybridization was performed to isolate novel messages expressed specifically in the early chick embryonic heart (Reese et al., 1999). cDNAs expressed in the stage 18 heart were subtracted from cDNAs expressed in the chick embryo minus the heart, sequenced, and blasted against NCBI sequence databases. Twelve out of the 120 clones were unknown sequences. A Northern blot analysis of heart tissue RNA and heartless embryonic RNA was probed with four of the novel clones isolated from the subtractive screen. The gene of interest in this chapter, called *hole* (H136), produced a common sized message in both tissues

and an additional, exclusive message in the heart (Figure 2). A second cloned, named *bves* (H164), will be addressed in the following chapters.

A stage 18 chick cDNA heart library was screened using a 200 bp probe amplified from the original *hole* clone. Two independent clones were isolated, sequenced, and blasted against sequence databases. The clones were novel and spanned a total of 3.6 kb, with 1.01 kb of overlapping, identical sequence (Figure 3). Protein translation predicted a 960 bp open reading

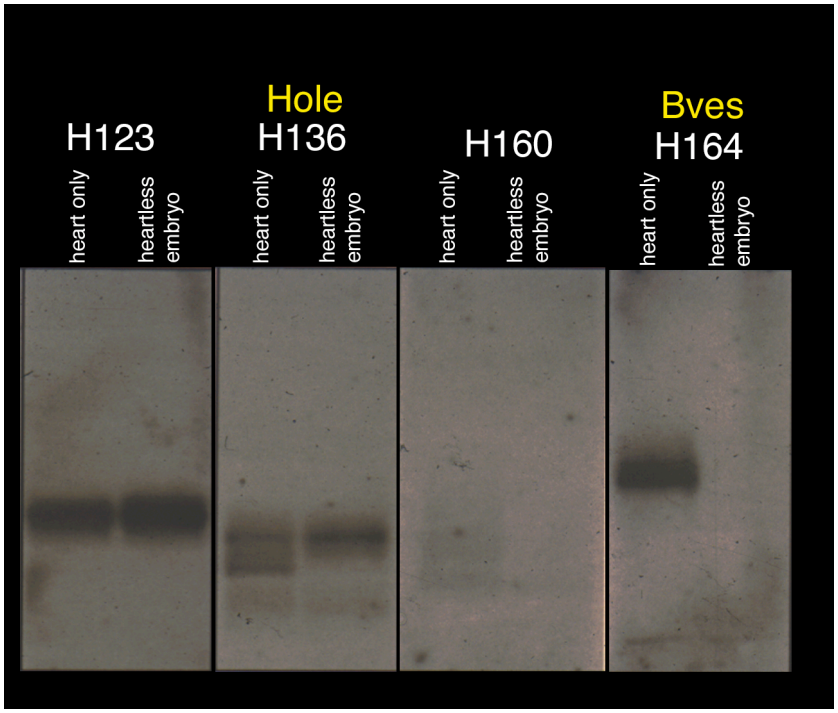

Figure 2. Northern blot analysis of expression of 4 isolated clones in stage 20 chick heart and heartless embryonic RNA. Clone H123 is expressed in both heart and heartless embryo, while H160 is expressed in neither. These both are examples of a false positive result from the subtractive screen and were not further investigated. Analysis of H136 *(hole)* expression revealed two transcript sizes expressed in heart RNA and one in heartless RNA. H164 (*bves*) expression is seen exclusively in the heart at the stage represented.

frame, which includes a potential methionine start codon accompanied by a Kozak sequence, CACC**ATG**GTG. The open reading frame is terminated by a stop codon and is followed by an 800 bp 3' UTR containing a poly-adenylation signal sequence, and preceded by a 1.8 kb 5' UTR. RT-PCR results (not shown) performed on heart RNA using several primers specific to the large 5' UTR proved that this 5' region was indeed included in the message. A genomic clone was isolated from a cosmid chick genomic library and partially sequenced. This clone contained the entire *hole* cDNA in one intronless exon (Figure 3), which further verified the validity of the 5'UTR sequence.

The chick cDNA sequence was compared with known sequences in the NCBI databases in order to determine if *hole* shared any sequence homology to other cDNAs. There was no sequence similarity to any known sequences. However, mouse ESTs from day 13.5-14.5 embryonic libraries were obtained from blasting chick sequences into the various EST databases. These sequences were used to screen a mouse embryonic day 14 heart cDNA library. Two clones were isolated from the screen and sequenced. The clones were 1.6 and 2.8 kb, sharing the first 1.6 kb of identical sequence, including a poly-A tail. The larger clone had 1.2 kb of sequence after the poly-A tail and I concluded it was a chimeric clone of no significance. The mouse sequence contains a 1.2 kb ORF including a potential start methionine and Kozak sequence 240 bp downstream, and a stop codon 960 bp downstream from the start site (Figure 3). This region shares 72% sequence identity with the chick ORF region and is followed by a 400 bp 3'UTR. The cDNA hole clone was used to probe a mouse lambda genomic library. One clone was isolated and partially sequenced. The 1.6 kb cDNA was present as one exon minus 27 bp 5'. Mouse genomic databases were searched and additional sequence was obtained. The 27 base pairs were found 2 kb upstream of the original exon (Figure 3). Additionally, human EST

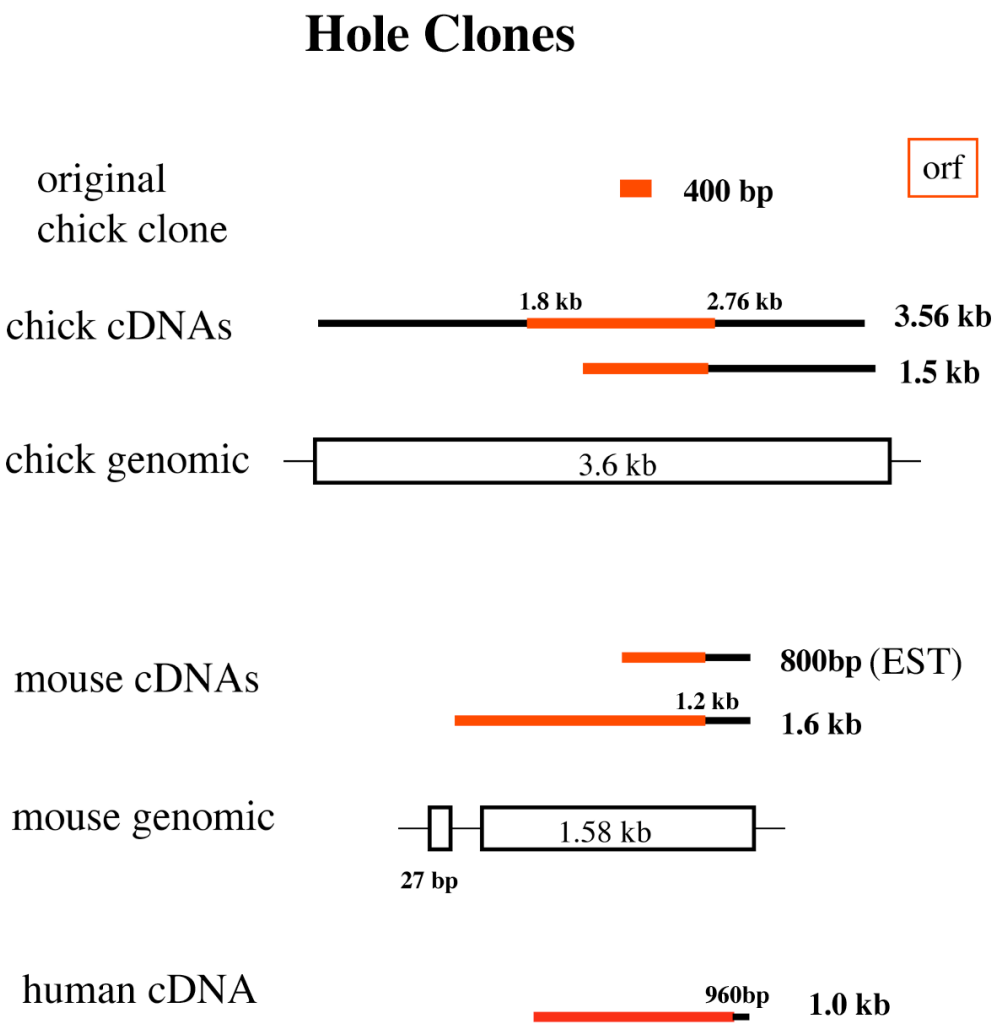

Figure 3. Schematic representation of *hole* cDNA and genomic clones isolated from chick, mouse, and human libraries. The original clone isolated from the heart subtractive hybridization was 400 bp and used to screen other libraries. Two different sized cDNA fragments, 3.56 kb and 1.5 kb, were isolated from a stage 18 chick heart cDNA library. Overlapping sequence was identical and totaled an open reading frame (orf) of 960 bp. *hole* EST from a mouse day 13.5-14.5 embryonic library, size 800 bp, was obtained from NCBI EST database and used to screen a day 14 mouse heart cDNA library. Two clones were isolated, totaling 1.6 kb with a 1.2 kb orf. A human EST was found on the EST database comprising 1.0kb total and 960 bp of orf. Chick and mouse genomic libraries were screened with respective cDNAs and resultant clones are illustrated. Red lines represent open reading frame.

sequences were obtained from the NCBI databases that show 87% identity to mouse sequence. The assembled human sequence includes a 960 bp ORF and a 108 bp 3'UTR.

Predicted translated products of chick, mouse, and human *hole* share a conserved potential methionine start site and coding sequence for 311, 317, and 318 amino acids, respectively (Figure 4). The Hole protein is 91% similar between mouse and chicken and 99% identical between mouse and human, with the most divergence occurring the c-terminus. Transmembrane prediction programs predict with 80-100% probability that the Hole protein contains six transmembrane (TM) spanning regions and an 87 amino acid C-terminus (Figure 5). While the number of TM domains most closely resembles that of calcium, sodium or potassium channels, a large loop is present between TM domains 4 and 5 of Hole, while these channels typically have a large P-loop in between domains 5 and 6 (Lehmann-Horn and Jurkat-Rott, 1999). Because this novel protein mostly consists of numerous TM domains and there are no other known domains or signals that would suggest protein function, the gene name *hole* is representative of the protein forming a hole in the membrane.

Northern blot analysis

In order to determine the message size of *hole* in the chick, as well as determine specifically in what tissues *hole* is expressed, Northern blot analysis was performed. Total RNA was isolated from the various tissues indicated in Figure 5, separated by gel electrophoresis and transferred onto PVDF membrane. The blot was probed with a 200 bp ^{32}P-labeled chick cDNA. Two messages, sized 3.6 and 3.3 kb, were detected in the heart tissue, while only the larger message was detected in the brain (Figure 6). There were no *hole* messages found in the liver, gizzard or skeletal muscle. These data support the initial result from the Northern analysis

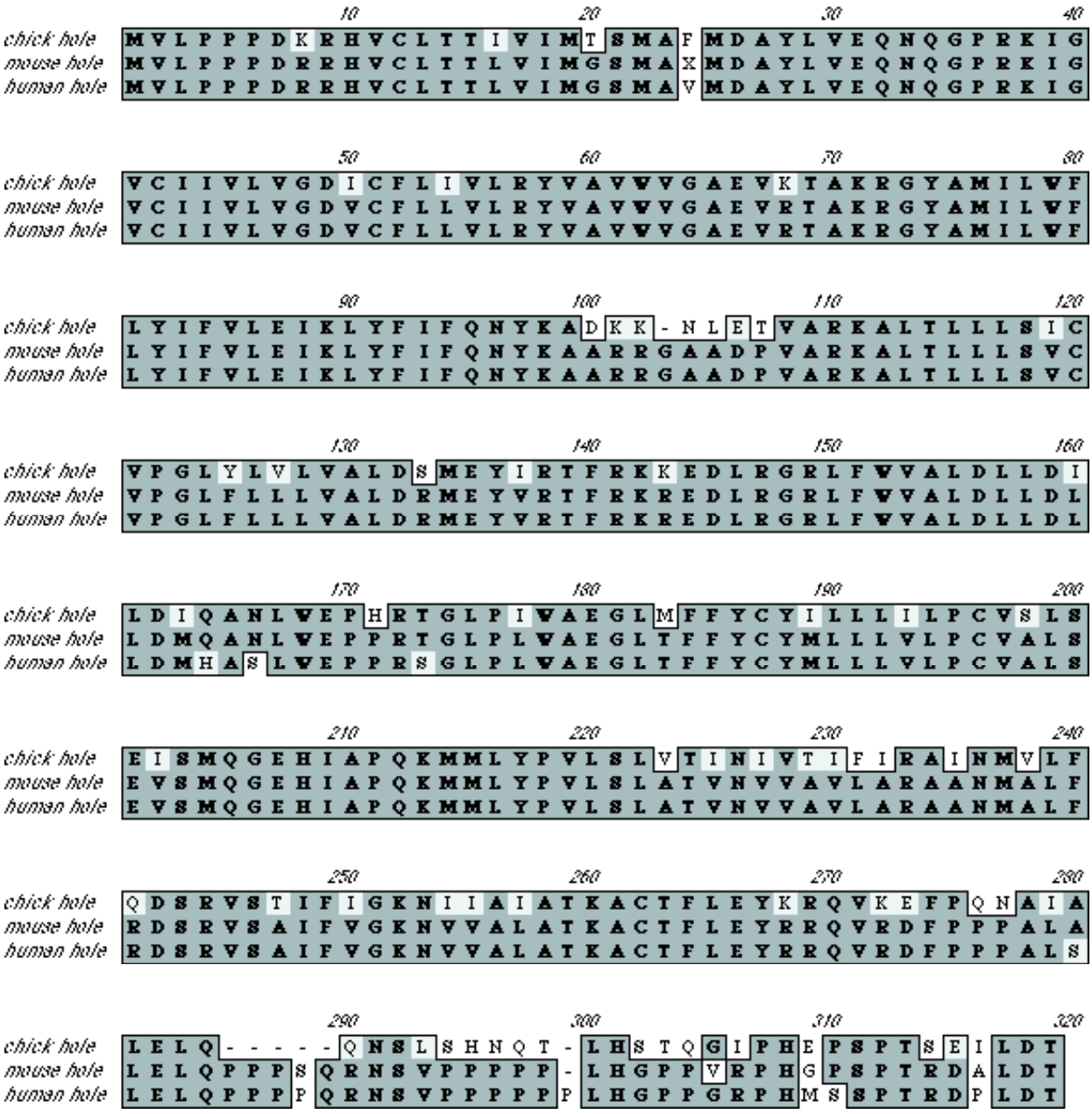

Figure 4. Protein alignment of the predicted amino acid sequences of chick, mouse and human Hole.

performed on the clones isolated from the subtractive hybridization. Using the initial *hole* clone (initially termed H136) as a probe, there are two messages found in the heart RNA and one message expressed in the whole embryo minus the heart (Figure 2).

Whole mount and radioactive *in situs*

In order to examine the precise spatial and temporal patterning of *hole* in the chick embryo, *hole* RNA distribution was detected by whole mount *in situ* hybridization. *hole* expression was examined in stage 4-25 chick embryos, which cover all the pertinent stages of morphogenetic heart formation. Embryos were probed with a DIG-labeled probe, which includes the ORF and

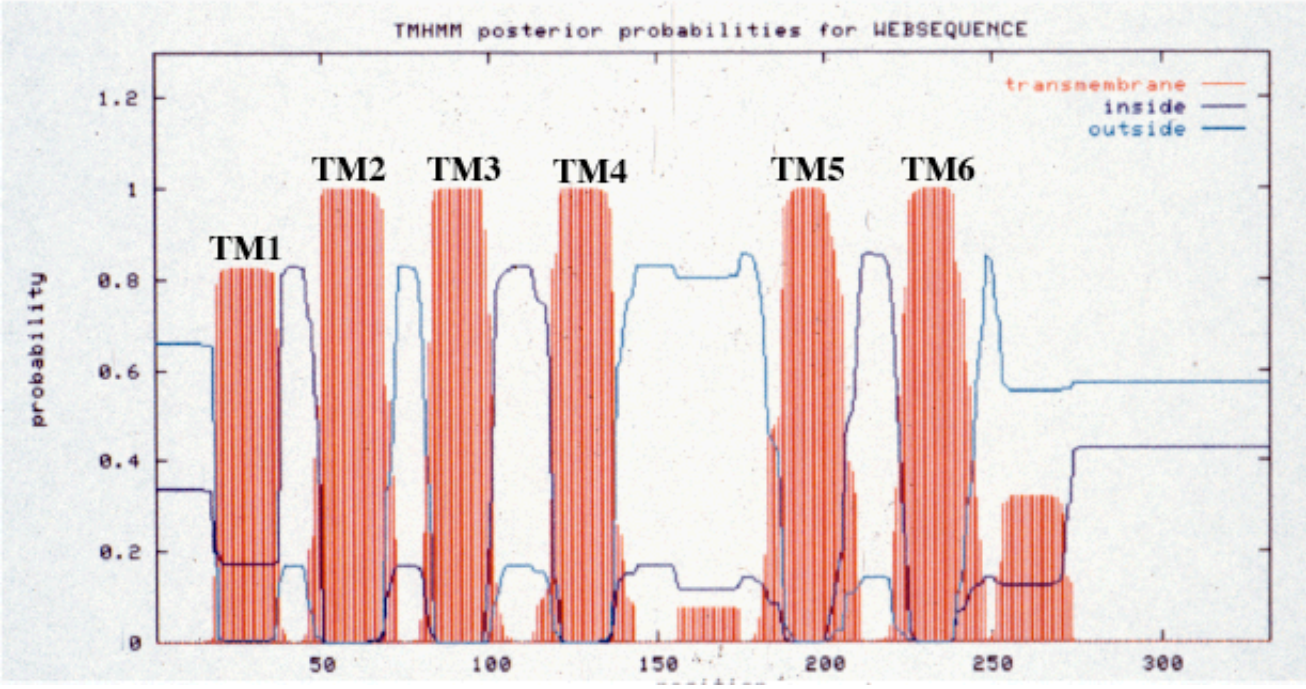

Figure 5. Transmembrane prediction of Hole protein sequence based on a Markov model for predicting transmembrane helices. The probability (y-axis) of amino acid residues (x-axis) being embedded in the membrane is represented in red. The purple line represents the probability of inter-transmembrane residues being intracellular and extracellular residues are shown as the green line. Note there is an exceptionally large extracellular loop between TM (transmembrane regions) 4 and 5.

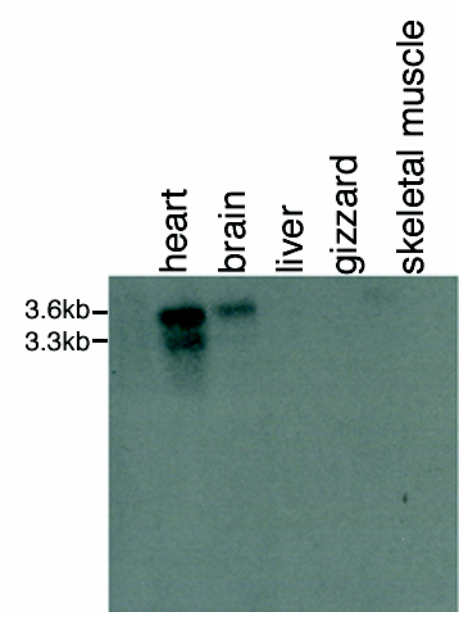

Figure 6. Northern blot analysis of day 10 chick tissues. Heart, brain, liver, gizzard and skeletal muscle tissue was probed with 200 bp *hole* cDNA. There are two transcript sizes, 3.3 and 3.6 kb, in the heart and one, 3.6 kb, in the brain.

3'UTR of the cloned chick cDNA. An alkaline phosphatase-conjugated anti-DIG antibody was used to detect *hole* RNA hybridization. Detection of *hole* RNA expression was seen as early as HH stage 4 in the anterior lateral heart-forming region of the embryo (Figure 7). Expression becomes more restricted to the cardiac precursor cells and the head fold in stages 4-6, and is later seen at the advancing edges of the fusing neural tube at stage 8 (Figure 7). As the heart tube fuses and loops, *hole* RNA is detected in both atria and ventricles (Figure 8A). Radioactive *in situ* hybridizations detected *hole* RNA throughout the myocardium of the heart during the stages shown (Figure 8F-J). Radioactive *in situ* hybridizations were performed on tissue sections in order to analyze embryos of later stages and eliminate nonspecific hybridization due to impermeable, thick tissue. As detected in the whole mount *in situs*, *hole* RNA is expressed throughout the myocardium during heart formation and maturation. (Figure 8).

In addition to the heart, *hole* RNA was detected in other tissues including neural ganglia and the developing limbs. In figure 9, *hole* RNA detection is seen in the trigeminal nerve ganglia in a stage 18 embryo whole mount *in situ*, as well as in stage 18, day 6, and 7 sagital and transverse sections. The expression of *hole* is also seen in the developing limb bud of the stage

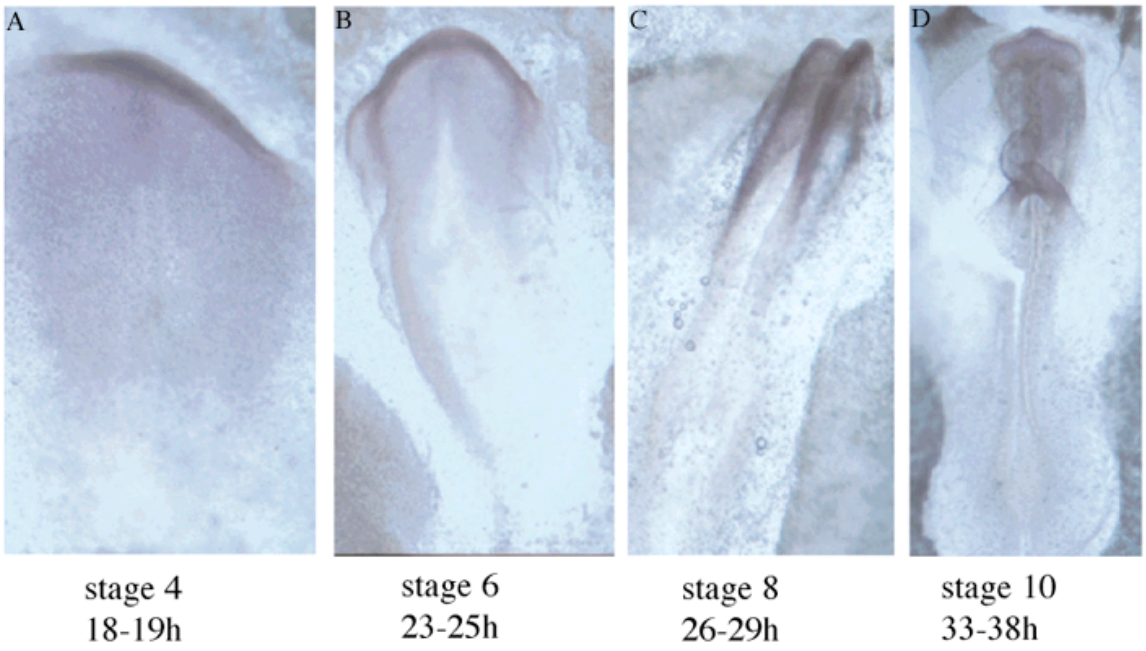

Figure 7. The detection of *hole* transcript in early chick development by whole mount *in situ* hybridization. *Hole* is broadly expressed in cardiac crescent (A, B), head fold (B), forming neural tube (C), and head and heart tissues at indicated stages of chick embryogenesis.

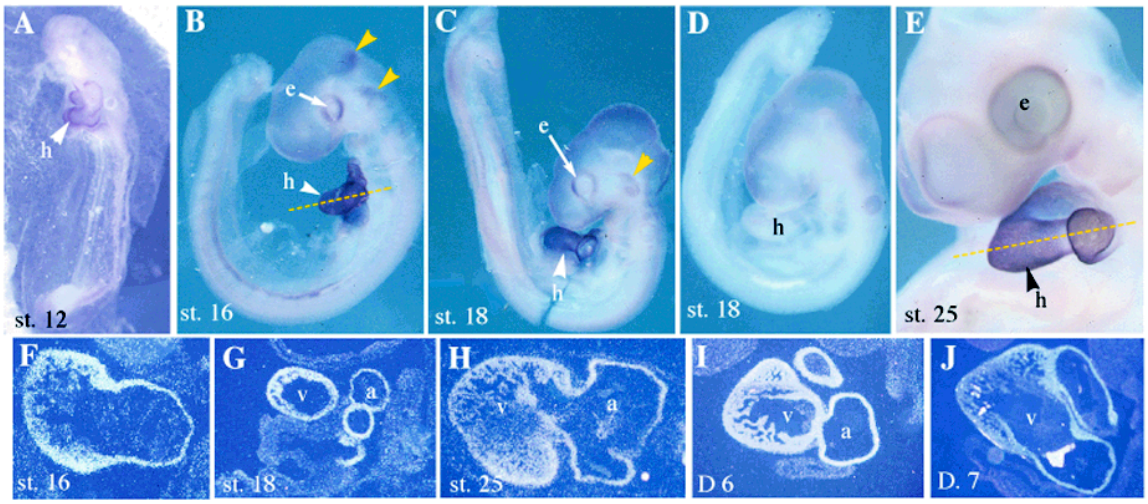

Figure 8. The expression of *hole* in the developing heart in stage 12 to day 7 chick embryos. Expression is observed in the heart (h) (white arrowhead), surrounding eye (e) (white arrow), and in patches in the mid-hind brain region (yellow arrowheads). (A) Ventral view of a stage 12 embryo. (B,C) Lateral views of stage 16 and 18 embryos. (D) The sense control at stage 18. (E) Lateral view of stage 25. (F-J) Localization of *hole* transcripts in stage 16 to day 7 developing heart by radioactive section *in situ* hybridization. The levels of the sections are indicated in panels B and E.

22 embryo and later in the dorsolateral tissue of the limb.

The expression of *hole* in the mouse embryo was examined throughout early development by whole mount *in situ*. Embryos stages 8.5-12.5 dpc were probed with the full-length DIG-labeled mouse cDNA. There was no expression of *hole* in the heart throughout these stages (Figure 10). However, the mouse displayed a strong neural expression pattern. From the earliest stage examined, *hole* expression is seen in the neural tube. Additional expression is observed in the interdigital tissue of the stage 12.5 limb (Figure 10). The divergence in *hole* expression pattern between the chick and mouse in unknown at this time.

Discussion

A novel heart enriched transcript called *hole* has been isolated from a subtractive hybridization screen, which selects for early expressed chick heart-specific gene products (Reese et al., 1999). Northern blot analysis reveals a transcript size of 3.3 kb specific to the heart and a transcript size 3.6 kb shared between the heart and brain tissue of day 10 chick. Mouse and human cDNAs have also been isolated and share high sequence homology with the chick cDNA. The predicted proteins are between 311-318 amino acids. A potential methionine start site and stop codon are conserved amongst all three species.

Analysis of the protein sequence predicts that Hole is a six transmembrane protein with a longer extracellular loop between transmembrane (TM) spanning regions 4 and 5. Computer analysis does not identify any known domains in the Hole protein. There are several families of voltage gated ion channels that do, however, share the six TM structure with Hole. Cardiac

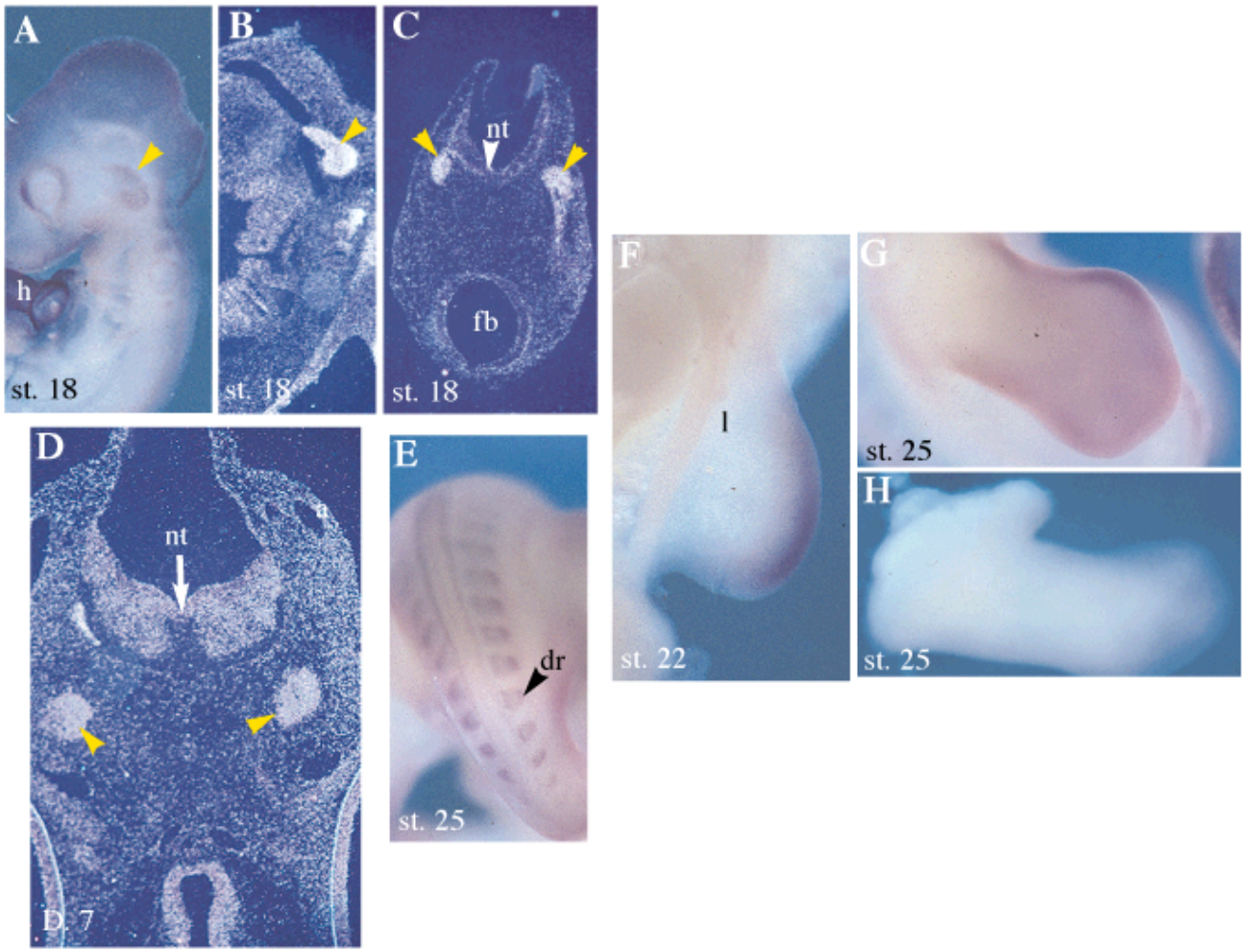

Figure 9. Localization of *hole* during the formation of chick brain and limbs. (A,B) Lateral view of stage 18 embryo by whole mount *in situ* (A) and radioactive section (B). (C) Transverse section through the brain of stage 18 embryo. Dorsal root ganglia are indicated by the yellow arrowheads. (D) Localization of *hole* transcripts in the brain of day 7 by section *in situ* hybridization is seen in several areas of the fore- and hind-brain regions. (E) Dorsal view of a stage 25 embryo, (dr) dorsal root ganglia. (F-H) *Hole* expression in the forming limb bud. (F,G) Ventral view of a stage 22 and stage 25 hindlimb. (H) The sense control of the limb at stage 25.

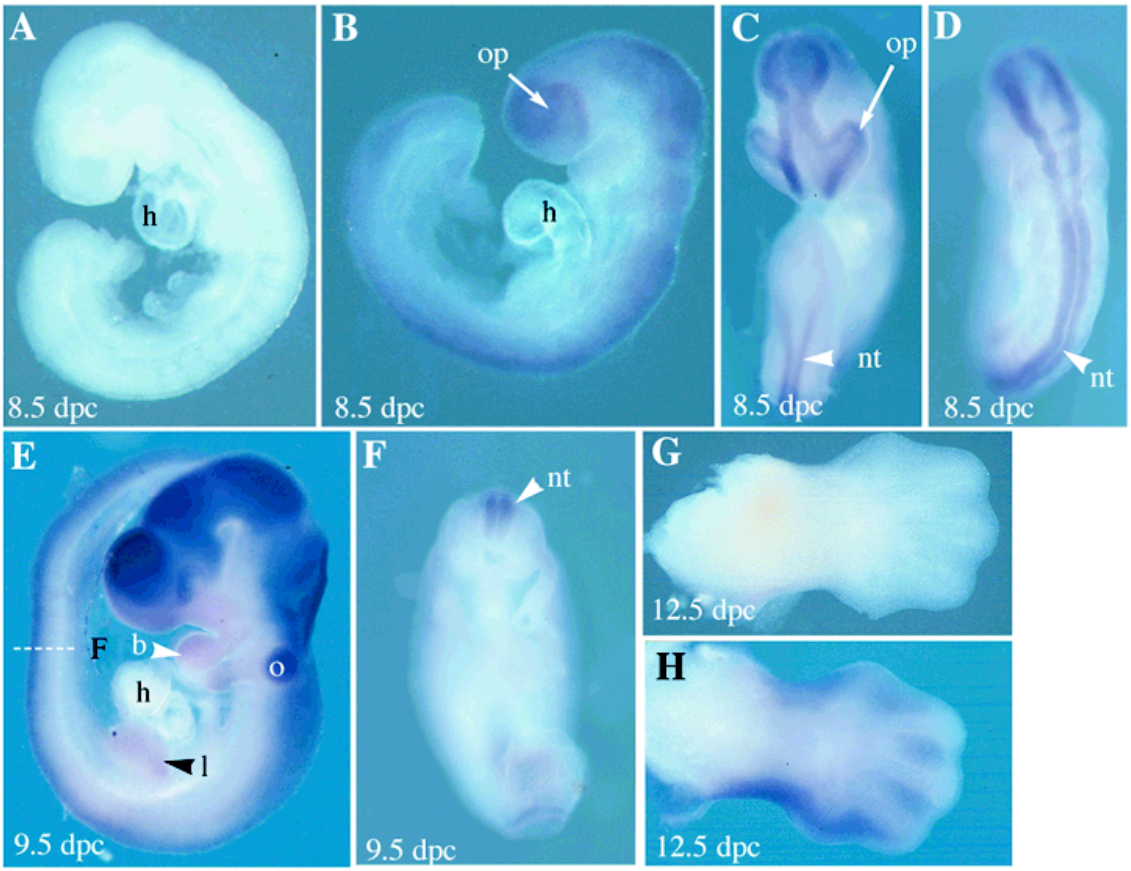

Figure 10. Localization of *hole* transcripts in 8.5 to 12.5 dpc mouse embryos. (A) Lateral view of a 8.5 dpc sense control. (B-D) *Hole* expression in the optic placode (op) and neural tube (nt) of a 8.5 dpc embryo, (B) lateral view, (C) frontal view, (D) dorsal view. (E-F) *Hole* expression in the neural tube (nt), forming brain, brachial arches (b) and limb buds (l) of a 9.5 dpc embryo. Expression is not seen in the heart (h). The level of staining in F is indicated in E (white dashed line). (G) The sense control of the limb at 12.5 dpc. (H) The expression of *hole* in the interdigit regions of the forming limb of a 12.5 dpc embryo.

potassium, sodium, and calcium channels are composed of four subunits of six TM spanning regions (Figure 11A-B) (Balser, 1999; Snyders, 1999; Striessnig, 1999). A larger extracellular "pore" loop, termed the P-loop, is located between TM region 5 and 6 of each of these channels. A set of four P-loops arranged in a circular array forms a pore (Figure 11B) through which the specific ions travel as they enter or exit the cell. Mutational analysis shows that specific domains and amino acid residues in the P-loop define the ion selectivity. Additionally important to ion channels function, TM 4 carries a positive charge due to the excess of basic residues and is a major component of the voltage sensor for gating (Lehmann-Horn and Jurkat-Rott, 1999).

Differences between the three types of channels do exist. Each of the four subunits of the potassium channel is translated as a separate product and the subunits are assembled together at the membrane post-translationally (Snyders, 1999). This differs from sodium and calcium channels where all four subunits are encoded by one gene (Balser, 1999; Lehmann-Horn and Jurkat-Rott, 1999; Striessnig, 1999). Additionally, the four P-loops in the potassium channel share identical sequence but are not homologous to any other known ion channels (Snyders, 1999). Each of the four P-loops of the sodium and calcium channel is unique, but highly homologous amongst species and to each other. Finally, mutational analysis has shown that each of the three ion channels contains a unique and conserved sequence that serves as a "selectivity filter" for ion specificity. The potassium channel has a unique sequence of (TxTTx)GYG in all four P-loops that is essential for potassium ion specificity (MacKinnon, 1995), while the calcium channel contains an essential glutamate residue in all four P-loops (Ellinor et al., 1995) and the sodium channel requires a lysine residue in only the third subunit of the P-loop (Figure 11C) (Heinemann et al., 1992; Perez-Garcia et al., 1997).

Comparison of the protein sequence and structure between Hole and other known cardiac ion channels proved to be nominal. Although Hole does have a larger extracellular loop region, it is located in between TM regions 4 and 5, whereas the large P-loop in the presented ion

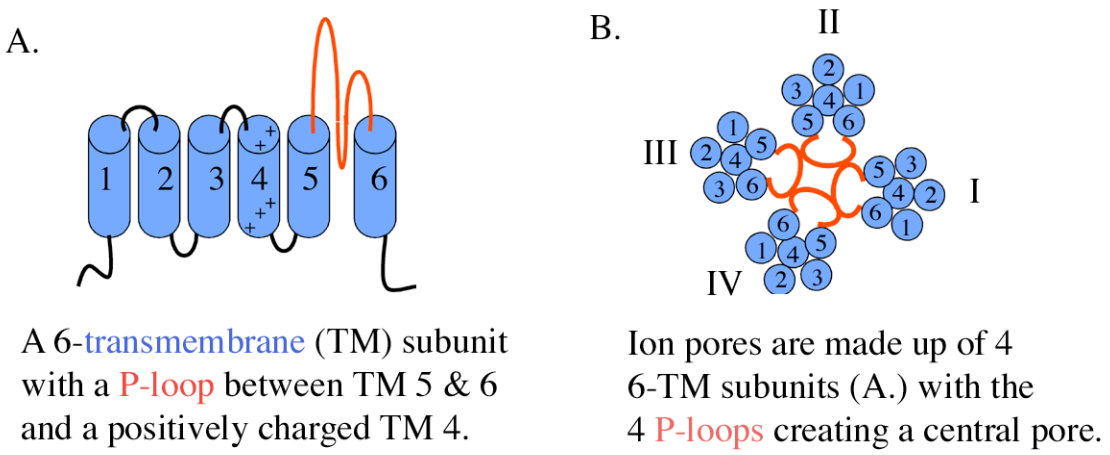

Figure 11. Schematic illustration representing the structure of cardiac calcium, potassium, and sodium ion channels. (A) Each subunit consists of 6-transmembrane domains with a long extracellular P-loop located between TM domain 5 and 6. (B) Each channel consists of 4 6-TM subunits with the P-loops forming an ion specific pore. (C) Conserved residues in the P-loops of the indicated ion channels designated ion specificity.

channels lay between TM region 5 and 6. This extracellular loop region in Hole contains 9 aspartic and glutamic acids, which are linked to calcium and sodium channel specificity. Similar to the potassium channel, the *hole* gene translates one six TM structure, unlike the calcium and

sodium channel gene that translates 4 subunits of 6 TM each. However, I have not conducted any studies to verify the significance of these similarities.

Predictions based on present data can be formulated. *Hole* is a novel gene product that shares no homology to any other gene family, but is highly conserved amongst species. The structure of the Hole protein is a six-transmembrane structure, similar to the configuration of cardiac ion channels. The dynamic expression pattern of *hole* in electrically coupled cardiac and neural tissue supports the hypothesis that Hole may define a novel ion channel family. This is supported by similarity in structure to known ion channels and the shared function of the two tissue types in conducting an electrical current. Additionally, the high degree of conserved sequence predicts that Hole is an important protein with a conserved function. While I terminated these studies due to technical difficulties, my work should provide the background for future studies.

CHAPTER III

XBVES REGULATES EPITHELIAL MOVEMENTS DURING GASTRULATION

Introduction

This chapter is a report on the *Xenopus laevis* homolog of the chick gene, *bves*, that was cloned from the subtractive hybridization screen from which *hole* was isolated. In this study, I have not only defined the expression pattern of *Xbves* in *X. laevis*, but I have also determined a phenotype directly attributable to the loss of the gene product in the developing embryo. This is the very first demonstration of its kind for *Xbves* and has laid the groundwork for numerous future studies. Unlike experiments with *hole*, the experiments described here were preceded by *bves* studies performed in the chick, mouse, and cell culture by members in our laboratory and by research groups at Technical University Braunschweig in Germany and at the University of Delaware. Based on a number of different studies, the resulting data allowed for the formulation of a hypothesis on *bves* function. Additionally, the establishment of morpholino technology and *X. laevis* Bves antiserum permitted detailed study of *bves* function.

This chapter will first describe the major events and movements during amphibian gastrulation. A brief review of previous *bves* studies will be outlined, followed by the rationale for choosing *X. laevis* as a model system. The results section will describe the cloning and expression pattern of *Xbves* mRNA and protein in the early embryo. Furthermore, the phenotype resulting from morpholino experiments where Xbves protein is reduced in the embryo will be presented. I will show how this phenotype results from an inhibition of epithelial movements

during gastrulation, and how this data supports our hypothesis that *Xbves* is important in maintaining the adhesive equilibrium necessary during epithelial migration.

Convergent/extension, epiboly and involution are some of the first and most fundamental movements of epithelia during embryogenesis (Gerhart and Keller, 1986; Hardin and Keller, 1988; Keller and Danilchik, 1988; Keller and Tibbetts, 1989; Keller, 1980). Proper epithelial migration is essential in establishing organizer regions and their resultant signals that regulate gastrulation and the formation of mesoderm (Keller and Danilchik, 1988; Keller et al., 1992; Wilson and Keller, 1991; Winklbauer, 1990; Winklbauer and Nagel, 1991). These movements are critical for positioning cells in their formation of germ layers in prelude to organ formation (Nieuwkoop, 1973; Shih and Keller, 1992; Winklbauer, 1990). Gastrulation involves the coordination of several distinct events driven by region-specific movements that are associated with a complex balance of spatially and temporally regulated adhesion. The beginning of gastrulation is marked by changes in the shape of bottle cells at the site of the blastopore (Hardin and Keller, 1988). These endodermal bottle cells invaginate in the marginal zone, permitting the marginal cells to involute through the blastopore lip and continue to pass into the interior as a sheet of cells. The involuting cells at the leading edge of the mesodermal mantle migrate along the inner surface of the blastopore roof towards the animal pole, forming the archenteron (Hardin and Keller, 1988; Keller and Danilchik, 1988). These sets of movement are driven by active repacking of the cells, where cells cooperatively form and align lamellipodia creating interdigitation of cells, and result in narrowing and elongation of tissue (Keller et al., 1992; Keller and Tibbetts, 1989). This forms the force necessary for the cells to converge toward the dorsal midline and extend along the antero-posterior axis, also known as convergent extension. During this time, the external epithelium in the region of the animal pole spreads to take the

place of the cell sheets that have turned inward (Keller and Tibbetts, 1989; Shih and Keller, 1992; Wilson et al., 1989). The epithelium of the animal hemisphere extends to cover the entire external surface of the embryo. This mechanism of epiboly is driven by an increase in cell number coupled with change of cell shape and integration of several deep layers into one (Keller and Tibbetts, 1989; Keller, 1980).

Dynamic expression of many types of adhesion molecules is associated with these three sets of movement during gastrulation. Migrating mesodermal cells on the blastocoel roof express integrins that bind to the extracellular matrix protein, fibronectin, covered along the roof (Beddington and Smith, 1993; Winklbauer, 1990). Cells undergoing convergent extension in the marginal zone express EP/C-cadherin and XB/U-cadherin (Kuhl et al., 1996; Lee and Gumbiner, 1995; Zhong et al., 1999), while the epiboly of the ectoderm depends upon E-cadherin (Levine et al., 1994). Therefore, we can conclude that cell adhesion molecules play a role in cell movements, both in cell adhesion and cell detachment, during early *X. laevis* embryogenesis that are vital for the proper formation of the three germ layers and continued normal development.

Bves/pop1a was independently cloned from avians and mammals (Andree et al., 2000; Reese and Bader, 1999; Reese et al., 1999). Andree et al. (2000) have identified three and two genes respectively in chickens and mice. They went on to show that splice variants differing primarily in their 5' and 3' UTRs and most N- and C-terminal coding regions are transcribed from these genes in these species. This gene family has been referred to as *popeye1-3* (Andree et al., 2000), however the accepted nomenclature for the first identified member of this family is Bves (Reese et al., 1999) (NCBI AF 124511). Computer modeling and biochemical analyses have suggested that Bves is an integral membrane protein with three hydrophobic domains (Andree et al., 2000; Knight et al., 2003; Wada et al., 2001). While variation in the number of

hydrophobic domains in different protein members of the *popeye* gene family appears to exist, two recent reports conclude that Bves/pop1a protein has a short extracellular N-terminus, three transmembrane domains with two small intervening loops and a long intracellular C-terminus (Andree et al., 2000; Knight et al., 2003) (Figure 1). While the sequence and overall structure of Bves/pop1a are highly conserved between species, computer modeling and database searches detect no structural homology with other proteins. In addition, no predicted functional motifs, outside the transmembrane domains, have been identified.

Expression studies of Bves/pop1a have not been conclusive to date (Andree et al., 2002; Andree et al., 2000; DiAngelo et al., 2001; Knight et al., 2003; Reese et al., 1999; Wada et al., 2001). *Bves/pop1a* was identified by subtractive hybridization as a transcript highly enriched in the embryonic heart (Reese et al., 1999; Andree et al., 2000). The transcript is strongly expressed in myocardium and skeletal muscle, as visualized by *in situ* hybridization and in brain, stomach, kidney, lung, and spleen, as shown by RT/PCR analysis (Andree et al., 2000). Examination of sectioned whole mount *in situs* reveals that the *bves/pop1a* transcript is also present in gut endoderm (Andree et al., 2000). *Bves* RNA is expressed in a broader range of tissues by RT/PCR in this same study and is also present in several cell types as ESTs (NCBI). The initial antiserum directed against chicken Bves protein recognized the gene product in the epicardium and smooth muscle of the coronary arteries but not in cardiac or skeletal muscle (Reese et al., 1999). Subsequent generations of anti-Bves/pop1a antisera and monoclonal antibodies from our laboratory detected the protein in cardiac myocytes, epicardium and arterial smooth muscle along with several epithelial structures in the embryo and a clonal epicardial cell line (Vasavada et al., 2004; Wada et al., 2001; Wada et al., 2003). DiAngelo et al. (2001) have reported a monoclonal antibody specific for avian Bves/Pop1a in cardiac muscle. To date, no

conclusive RNA or protein studies exist. While further examination of the expression pattern of this novel gene family is required, the emerging picture is that Bves/Pop1a is highly expressed in striated muscle but is also present in various epithelial cells of the embryo and adult.

Detection of the Bves protein in tissue sections of developing embyros and cell culture by indirect immunofluorescence reveals a dynamic subcellular distribution of Bves. During epicardial and coronary artery formation, Bves protein accumulates in the cytoplasm of migrating mesenchymal cells and colocalizes with Golgi specific antibodies (Reese et al., 1999; Wada et al., 2001). Similar cytoplasmic distribution is detected in cornea epithelial cells that delaminate from the epithelial sheet after wounding and migrate as single cells (Ripley et al., in press). Upon formation of epithelia both in the heart and cell culture, Bves translocates to the cell surface (Reese et al., 1999). Membrane staining of Bves is seen in the formation of many epithelial structures including the gut, kidney, eye, and epidermis, as well as various adult tissues (Osler and Bader, 2004).

Functional analysis of Bves/Pop1a has just begun, and is inconclusive. Bves traffics to points of cell-cell contact early in the generation of epithelial sheets and later colocalizes with cell adhesion proteins (Wada et al., 2001). Transfection of chick *bves* cDNA into nonadherent L-cells confers homotypic adhesive behavior (Wada et al., 2001). Deletion analyses are currently underway to pinpoint the domains responsible for cell-cell adhesion. Serial deletion of the C-terminus of Bves followed by immunoprecipitation had determined that amino acids between 251-284 in the chick protein are essential for interaction between Bves molecules. Spot blot analysis (SPOTS) of a series of 11 amino acid peptides spanning the chick bves protein identifies a 11-13 amino acid domain located in the C-terminus within the core domain described

above that appears to mediate C-terminus interaction (Kawaguchi, personal communication) (Figure 1).

Andree et al. (2003) have recently reported that the *popeye1* gene mouse knockout has no embryonic phenotype in any cell or tissue type, but shows a delay in skeletal muscle regeneration, possibly due to an initial inhibition of myoblast fusion. Redundancy of *popeye1* and *2* expression may account for the lack of an overt phenotype (Andree et al., 2002; Andree et al., 2000). It should be noted that a thorough analysis of all embryonic developmental and adult regeneration processes is a prodigious task. Clearly, *bves* function is unknown especially in an *in vivo* model and further functional analysis is important to determine the role(s) of this gene family at any point in development.

The *X. laevis* embryo provides a system that allows us to examine the role of gene products in dynamic cell processes, such as gastrulation. The *X. laevis* embryonic model is preferred over other model systems to examine cell-cell adhesion molecules during early embryogenesis for several reasons. First, *X. laevis* embryos develop externally, meaning they can be fertilized and raised in a petri dish. Second, the size of the earliest staged embryo is large enough to be seen with the naked eye and is strong enough to maintain its structural integrity. This is significant because it allows us to manipulate the embryo at any stage, including direct injection of material into the cell. Manipulations include injection of RNA, blocking protein translation using antisense/morpholino primers, explant transplantation and creating transgenic frogs. Fate maps at early cleavage, gastrulation, and neural plate stages have been generated that allow us to determine the origin of a descendent cell population, thus targeting a specific developmental process (Hausen and Riebesell, 1991; Keller, 1991). Because of the features of this model system, we are able to assess the effects of genetic and experimental manipulation on

the embryos as they continue to develop *in vitro*. Therefore, we can use the *X. laevis* system to examine the potential role of the newly cloned *bves* family member, *Xbves,* in adhesion and development.

Morpholino injection is an effective method used to investigate gene function in the *X. laevis* embryo (Heasman et al., 2000; Nasevicius and Ekker, 2000). Morpholinos inhibit specific protein production in the embryo and the resultant phenotype is assessed for developmental defects. Morpholinos have replaced the traditional antisense oligos by enhancing specificity, targeting, molecular nuclease resistance, and decreasing toxicity. Morpholino oligonucleotides are assembled from four different morpholino subunits, each of which contains one of the four genetic bases (adenine, cytosine, guanine, and thymine) linked to a six-membered morpholine ring by non-ionic phosphorodiamidate intersubunit linkages (Summerton and Weller, 1997), and create a "loss of function" effect by preventing translation of RNA. The effectiveness of a ß-catenin specific antisense morpholino injected at 2-cell stage has been shown to block translation until the neurula stage (Heasman et al., 2000), thus displaying significant morpholino stability. In addition, the injection technique used to deliver morpholino oligomers allows us to control which cells and at what developmental stage we want to target.

There are numerous examples of transcript blocking by morpholino injection into *X. laevis* embryos, including signaling, cell adhesion, and cell sorting molecules (Branford and Yost, 2002; Dibner et al., 2001; Heasman et al., 2000; Heasman et al., 2001; Houston and Wylie, 2003; Spokony et al., 2002; Tan et al., 2001). Heasman *et al.* (2000) showed that morpholino oligos blocked *β-catenin* translation when injected into the two-cell embryo, thereby blocking dorsal axis formation. The phenotype was partially rescued by injection of *β-catenin* mRNA lacking morpholino-targeted sequence. A second example includes the morpholino inhibition of

a superfamily cadherin called Axial Protocadherin (AXPC), normally expressed in the notochord at neurula stage. When injected with a morpholino against AXPC, embryos display an interruption of sorting of prenotochord cells and normal axis formation (Kuroda et al., 2002). Morpholinos can effectively block protein translation throughout several stages of development, allowing the *X. laevis* embryo to develop in the "absence" of a functional gene product so that the mutant phenotype can be assessed.

Several findings contributed to my decision to use the *X. laevis* in order to determine *bves* function in early embryogenesis. First, the discovery of *bves* ESTs in oocyte, cleavage, gastrulation, and neurula stage *X. laevis* libraries indicates that the *bves* transcript is expressed in early embryogenesis and signifies a potential role at these stages. Second, early *X. laevis* development is an ideal model because it allows for examination of fundamental processes in a controlled system. Third, previous data point to *bves* having an adhesive function in epithelia. *X. laevis* gastrulation is composed of a series of epithelial movements, and well-established techniques have been developed to examine these migration patterns in frog embryos. Lastly, studies using morpholino technology have been successful in knocking down targeted transcripts in *X. laevis* embryos. The resultant phenotypes seen in embryos deficient of specific cadherin adhesion molecules have been indicative of their adhesive function.

As a portion of my dissertation research project, I demonstrate the presence of *Xbves* mRNA and protein during the earliest phases of *X. laevis* development, suggesting a function for this protein in early embryogenesis. Morpholino disruption of Bves activity in early *X. laevis* embryos demonstrates that this protein is essential for the completion of gastrulation, resulting in termination of development and embryonic death. *In situ* hybridization analyses of organizer specific and mesodermal specific markers show that induction of these tissues is not affected in

morpholino-injected embryos, but migration of these cell populations during gastrulation is inhibited. Unlike in chick embryos, in *X. laevis* gastrulation migrating cells move over the surface of the embryo, involute and travel inside the embryo as a mostly intact epithelial sheet. Therefore, *X. laevis* gastrulation is an ideal model system to test our overall hypothesis that Bves plays an essential adhesive role in epithelial movement and morphogenesis during development.

Materials and Methods

Animals and cell lines

Adult *X. laevis* were obtained from commercial sources. Fertilized eggs were produced by standard methods (Danilchick et al., 1991) and staged according to Nieuwkoop and Faber (Hubrecht-Laboratorium (Embryologisch Instituut) et al., 1967). The A6 *X. laevis* kidney epithelial cell line was obtained from American Type Culture Collection (ATCC; Rockville, MD) and grown according to ATCC protocol. L6 mouse fibroblasts were maintained according to published methods (Thoreson et al., 2000). CHO cells were obtained from ATCC and transiently transfected with FLAG tagged *Xbves* and control plasmids using Fugene (Roche) reagent according to manufacturer's protocol.

cDNA cloning and antibodies

EST database searches revealed an expressed tag in a two-cell *X. laevis* library. Primers (5': CCTGTCACTGACACAAGTAAC, 3': CCCAGTAAGTCGATTGAATAGC) were designed and the sequence cloned from a tailbud library (the gift of Dr. Chris Wright). The resultant 500 bp cDNA was used as a probe to screen the tailbud library and a dorsal lip, and oocyte stage library (gifts from Drs. Chris Wright and Bruce Blumberg) and a total of 8

overlapping cDNAs were cloned comprising the entire 3' UTR, coding region and 55 bases of 5' UTR. This sequence has been deposited in the NCBI database (AF 527799). These were the only *Xbves* or *Xbves*-related sequences isolated after screening 10^8 independent clones. Two peptide antisera (Ab1:CENWREIHHLVFHLANT and Ab2: KLYSLNDPTLGKKRKLDT) were generated in rabbits (Biosynthesis) and affinity purified with the Pierce SulfoLink Kit using manufacturer's methods. Only Ab2 showed immunoreactivity in both A6 cell culture and embryonic tissue sections, and was used for the experiments in this paper. Anti-pan cadherin was also used in these studies according to methods described in the literature (Izutsu et al., 2000).

RT-PCR

mRNA was isolated from various embryonic stages using Trizol reagent according to manufacturer's instructions. RT-PCR analysis was performed using primer set: 5'ATGAAGGTGTCCTACCGAGGCCAT and 3'CAGTGTGGGATCATTGAGCGAGTA (266 bp product) and the Titanium RT-PCR kit (Clontech). Thermal conditions were followed according to manufacturer's instructions with the exception of an annealing temperature of 58° C and extension time of one minute. The polymerase/reverse transcriptase (RT) mixture was excluded from the negative control reactions and Taq polymerase (Promega) with no RT was added.

L-cell aggregation assay

Mouse fibroblast L-cells were stably transfected with full-length FLAG tagged *Xbves* cloned into pCIneo vector (Promega) containing a CMV promoter. Nontransfected, vector only-

transfected and *Xbves* transfected L-cells were tested for adhesive activity using the standard hanging drop suspension assay according to Thoreson et al. (2000). The ratio of number of cells in aggregates vs. the total cell number was tabulated and summarized by graph formation. Statistical analysis was determined using GraphPad Prism 3.0 (GraphPad software, San Diego, CA). All values are reported as mean ±SEM, unless otherwise indicated.

Whole mount *in situ* hybridization and immunochemical analyses

Whole mount *in situ* hybridization analysis was conducted according to published methods (Harland, 1991) with specific modifications communicated by the author. *Xbra*, *goosecoid*, and three *Xbves* probes bp 70-670 (5'), 870-1210 (3') and full-length 1-1738 were DIG labeled and hybridized to experimental or control embryos. Following substrate color reaction, embryos were post-fixed in Bouins, bleached for 1-2 hrs, and stored in methanol.

To characterize anti-Xbves antisera, immunofluorescence was conducted on A6 cells and transiently transfected CHO cells. Cultured cells were washed in PBS, fixed in 70% methanol for 10 minutes followed by extensive washing in PBS and blocked in 2% BSA/PBS for one hour. Anti-Xbves and anti-FLAG (Sigma) were reacted with samples overnight at 4°C for double indirect immunofluorescence analysis. Cells were then washed with PBS and incubated with the appropriate secondary antibody and DAPI at the manufacturer's suggested dilution. Tissue sections of *X. laevis* embryos were prepared according to published methods (Fagotto and Gumbiner, 1994). Immunochemical reactions and washings were conducted as described for cultured cells, except tissue sections were fixed in Histochoice (Amresco) instead of 70% methanol. Pre-immune serum, no first antibody and antibody depletion by peptide competition were performed and all were negative.

Oligonucleotides and mRNAs

Three antisense morpholino oligonucleotides were synthesized (Gene Tools) against *Xbves* 5'UTR and **ATG** start site (Xbves MO#1:**AT**CTTTCTTATACCTGGATGTGCAG, Xbves MO#2:CTTTCAGTAGT**CAT**CTTTCTTATAC, Xbves MO#3:ATGAATATGCTTTCAGTAGT**CAT**CT). Morpholinos were dissolved in RNase free water according to manufacturers instructions. Each of the morpholinos was injected at 5nl into both cells of the 2 cell embryos at varying concentrations. Only injection of MO#1 showed an inhibition of development, specifically gastrulation, and I concluded MO#2 and MO#3 to be ineffective at blocking the *Xbves* transcript. Therefore, the following studies represent injection of MO#1 at a concentration of 40ng into one or both cells at the 2-cell stage, unless otherwise indicated. The *Xbves* rescue plasmid excludes 5'UTR and begins with the start ATG codon. This plasmid excludes the MO#1 target sequence found solely in the 5'UTR. mRNA was synthesized by mMESSAGE mMACHINE (Ambion), and quantified by spectrophotometry. Rescue experiments were carried out by co-injection of 50pg rescue mRNA and MO#1 into both cells of the 2-cell embryo.

Results

***Xbves* cloning**

The evidence of a *bves* family member existing in *X. laevis* was first revealed from the EST database. EST clones from oocyte, 2-cell, gastrulation, and neurulation staged *X. laevis* libraries showed high homology to *bves* family members of other species. PCR primers were designed for these sequences and a 300 bp probe was constructed to screen a tailbud-staged cDNA *X. laevis* library. Three independent clones were isolated and sequenced. Aside from

varying 5' truncations (55 bp and 160 bp), all clones contained identical sequence totaling 1760 base pairs that include a 55 bp 5'UTR, 1185 bp of coding sequence and a 520 bp 3'UTR ending with a poly-A tail. The translated sequence encodes for a novel 338 amino acid protein, initiated with a methionine start site, which we have termed *X. laevis* Bves (Xbves). To determine whether there are additional *bves* family members in *X. laevis* or different isoforms expressed throughout early development, oocyte stage and gastrulation (anterior dorsal lip) stage cDNA libraries were screened using a 200 bp mid-region probe. Five independent clones were isolated from these libraries. The sequence of these clones was identical to those originally isolated, with the oocyte clones sharing the 55 bp 5'deletion and the gastrulation clones containing the full-length sequence. While these results do not determine whether additional *bves* family members or isoforms in *X. laevis* exists, it is evident that the one family member isolated from three separate *X. laevis* libraries is a prominent form of *bves* in *X. laevis* and this member, *Xbves*, became the focus in the following studies.

Xbves structure and adhesive function is conserved

The derived amino acid sequence predicts that the overall structure of Bves/Pop proteins with a short N-terminus, three hydrophobic domains and a long C-terminus, is conserved in Xbves. Xbves protein shares over 90% amino acid similarity with mouse and chick Bves (Figure 12). Still, significant variation in amino acid sequence exists in the N-terminus from amino acid residues 2-28 and in the extreme C-terminus (316-338). Exhaustive searches and computational

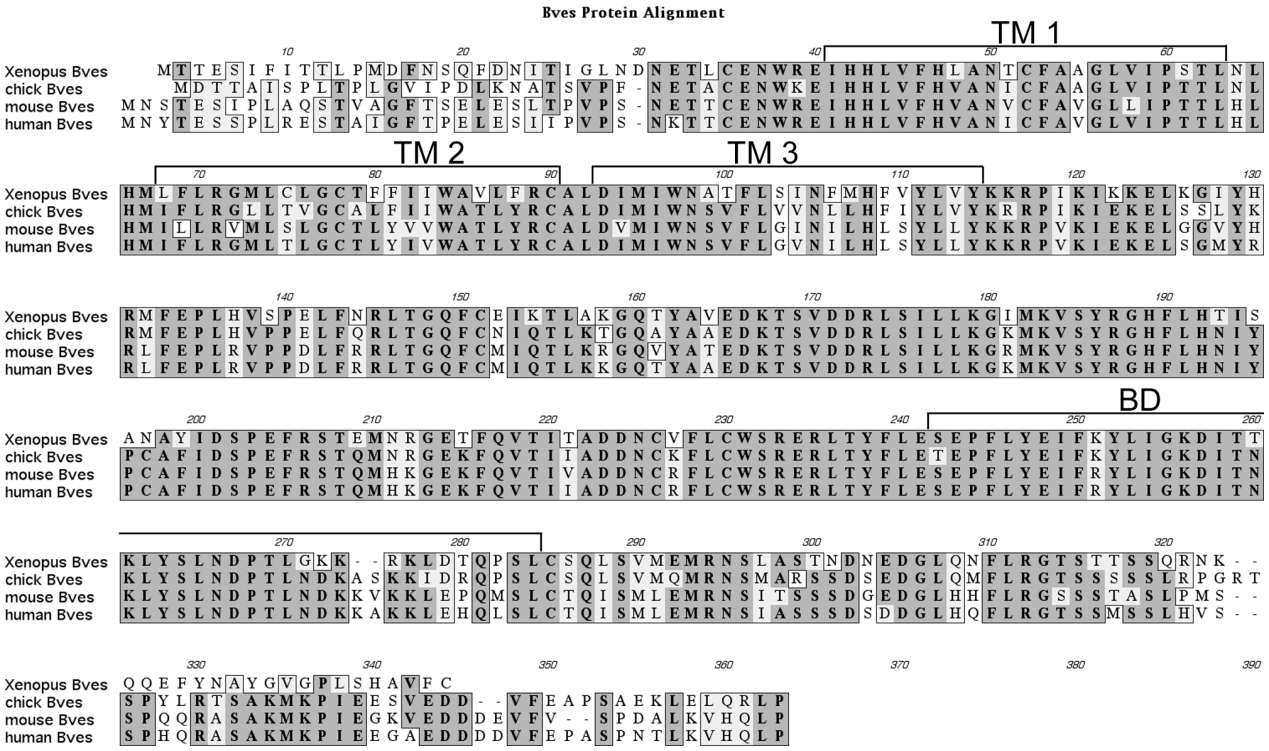

Figure 12. Protein alignment of the predicted amino acid sequences of *X. laevis*, chick, mouse and human Bves. Brackets denote the three predicted transmembrane (TM) regions and the predicted homophilic binding domain (BD).

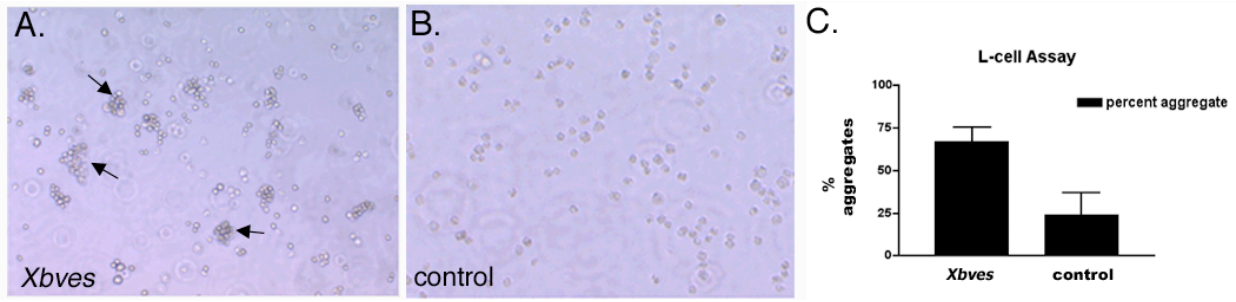

Figure 13. *Xbves* transfected L-cells confer adhesiveness. L-cell aggregation assay of *Xbves* (A) transfected L-cells and control (B) L-cells. (C) *Xbves* transfected L-cells show a 42% increase in number of aggregates formed compared with control cells.

analyses predict that Xbves harbors no known functional protein motifs and no homology to other protein sequences in the database.

We have reported that chick Bves confers adhesive behavior to non-adherent cells (Wada et al., 2001). To determine whether the same functional activity was conserved with Xbves, full-length FLAG tagged *Xbves* cDNA was transfected into L-cells and cell adhesion analyses were conducted. As seen in figure 13, *Xbves*-transfected L-cells readily adhere to each other, forming a statistically significant number of aggregates compared to control cells (66.83±3.45 vs. 24.00±4.18; $p<0.001$ by Student's t-test). These data demonstrate that while variation in the most N- and C-terminal sequences of Xbves protein exists, the binding domain in the C-terminal tail (Figure 1 and Figure 12) is similar to chick, thus suggesting the conservation of adhesive function in Xbves.

In accordance with previous studies, I also predicted that Xbves protein should traffic to the cell membrane as cells make contact and remain at the cell surface as cells adhere. To determine whether Xbves is detected at the cell surface, A6 kidney cells were grown *in vitro* and the subcellular distribution of Xbves was analyzed. In adherent A6 cells, Xbves is seen at the cell surface and colocalizes with pan-cadherin at points of cell-cell contact (Figure 14A-C). However, Xbves is not seen at the cell surface in individual A6 cells (data not shown). Additional intracellular Golgi staining with anti-Xbves mirrors that reported in mammalian cells (Wada et al., 2001). The A6 cell immunofluorescence, along with analysis of transfected CHO cells, also serve as a control for our immunochemical reagents. Experiments with *Xbves*-transfected and control CHO cells are provided and demonstrate the specificity of antiserum reactivity for Xbves protein (Figure 14D-E). Additionally, preimmune and no first antibody controls are negative for membrane staining (data not shown).

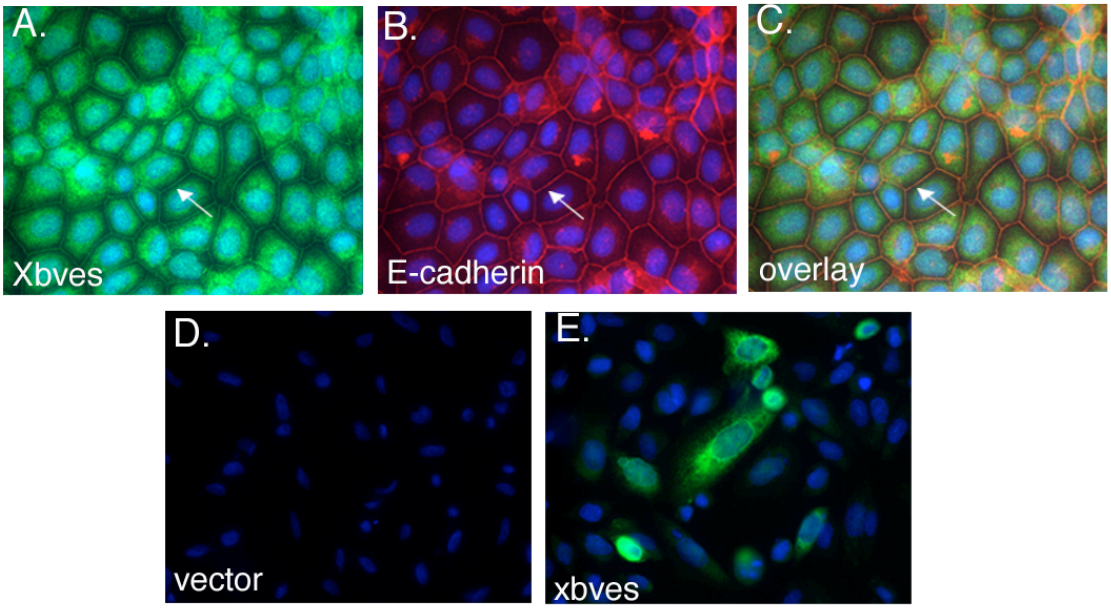

Figure 14. Immunocytochemical analysis of Xbves. (A-C) A6 *X. laevis* kidney epithelial cell show immunoreactivity with anti-Xbves (A, green), anti-pan cadherin (B, red). Overlay of anti-Xbves and pan-cadherin is shown in C. (D-E) Immunofluorescence analysis of CHO cells transfected with pCI-Neo vector only (D) or *Xbves* full-length construct (E) with anti-Xbves. DAPI nuclear stain is shown in blue.

Bves is expressed during the earliest stages of amphibian development

To analyze *bves* expression throughout the early stages of *X. laevis* development, RT-PCR was conducted on *X. laevis* mRNA prepared from embryos at selected stages of development. *Xbves* specific primers detected a message in oocyte, cleavage, gastrulation, and neurulation stage RNA, indicating that the *Xbves* message is supplied maternally until mid-blastula transition (MBT) and zygotically after MBT (Figure 15). Control experiments included no reverse transcriptase (RT), demonstrating the RNA dependence of the reaction.

To analyze more thoroughly the temporal and spatial patterns of *Xbves* expression, we conducted *in situ* hybridization analyses of *X. laevis* oocytes and embryos. *Xbves* transcripts were clearly observed throughout the unfertilized egg (data not shown). These data were not unexpected, as *Xbves* ESTs have been reported in *X. laevis* oocyte libraries. Interestingly, the

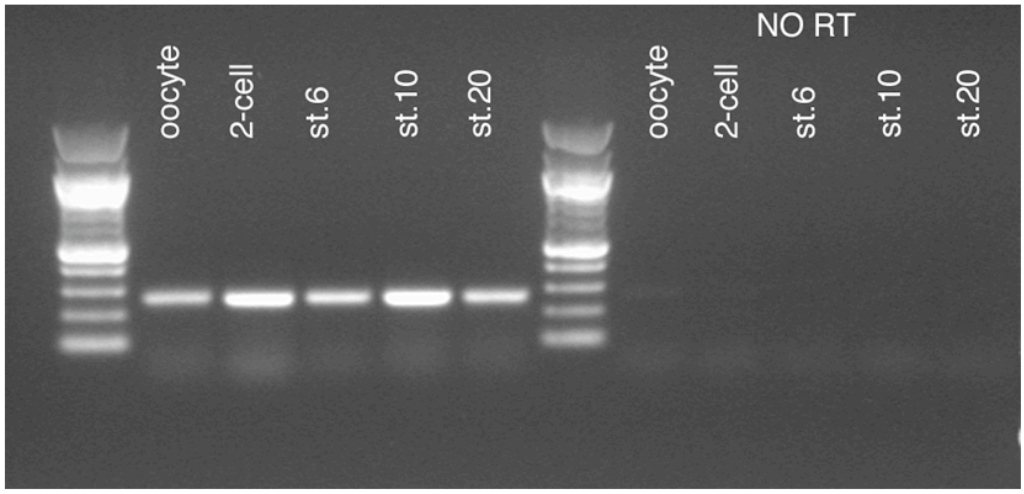

Figure 15. RT-PCR analysis of *Xbves* expression in *X. laevis* embryonic RNA. Negative control included reactions with no reverse transcriptase (RT) added.

distribution of *Xbves* mRNA changed in the two- and four-cell embryos, as hybridization was concentrated toward the animal pole (Figure 16A-F). As cleavage continued, the smaller cells of the animal pole remained most strongly positive for the *Xbves* probe as compared to the larger, yolk filled vegetal cells. A distinct border of *Xbves* expression can be seen at the equator of the cleavage stage embryo (Figure 16C,F, arrows). During gastrulation (stages 10-12), all animal cells are positive for *Xbves* and with the establishment of the blastopore, a clear distinction between positive staining of surface cells and negative staining of yolk plug cells is apparent (Figure 16G-H). With elongation of the embryo from stages 12.5 to 35, *Xbves* expression